

Perfect and broad absorption by the active control of electric resonance in metamaterial

N V Dung¹, P V Tuong^{1,2}, Y J Yoo¹, Y J Kim¹, B S Tung¹, V D Lam²,
J Y Rhee³, K W Kim⁴, Y H Kim⁵, L Y Chen⁶ and Y P Lee¹

¹Department of Physics, Quantum Photonic Science Research Center and RINS, Hanyang University, Seoul, 133-791 Korea

²Institute of Material Science, Vietnam Academy of Science and Technology, Hanoi, Vietnam

³Sungkyunkwan University, Suwon, Korea

⁴Sunmoon University, Asan, Korea

⁵Infovion, Seoul, Korea

⁶Fudan University, Shanghai, People's Republic of China

E-mail: ylee@hanyang.ac.kr

Received 10 October 2014, revised 11 February 2015

Accepted for publication 11 February 2015

Published 27 March 2015



CrossMark

Abstract

Anti-oscillating plasmas have been the key to perfect absorption induced by magnetic resonance. This is an achievement in recent research on metamaterials (MMs), especially in GHz and the lower-frequency regions of electromagnetic waves. Here, a comprehensive view of perfect absorption is introduced by means of both magnetic resonance and electric resonance in meta molecules. A conventional metal-dielectric-metal MM absorber is proposed to obtain dual-band perfect absorption. It is clarified that the mechanism of dual-band absorption is due to fundamental (at 7.2 GHz) and third-order (at 18.7 GHz) magnetic resonances. Finally, we develop triple-band absorption by integrating resistors in to the MM absorber. The electric resonance, under the presence of resistors, matches the impedance of the MM absorber with the air at 13 GHz and gives rise to the new absorption band, with absorption higher than 90%.

Keywords: electric resonance, perfect absorber, multi-plasma, metamaterial

(Some figures may appear in colour only in the online journal)

Perfect-absorption (PA) metamaterials (MMs), which are electromagnetic (EM) blackbodies under the concept of artificial subwavelength materials occupy an important position in EM and photonic research [1, 2] because of their possible applications in plasmonic sensors [3, 4], capturing solar energy [5], wireless power transfer [6], EM-wave camouflage [7], and so on. The first metamaterial absorber (MA) proposed by Landy *et al* was exploited for both magnetic and electric resonances to manipulate the effective parameters, which simultaneously satisfied impedance matching with the outside environment and proper loss enhancement [8]. However, the existence of transmission is a disadvantage of the single-layer MM. Therefore, MAs using the conventional scheme have effectively used a sandwich structure consisting of a periodic metallic pattern, a dielectric substrate, and an EM-wave-preventing metallic plane [1–3, 5, 6, 9, 10]. A typical MA sheet was used for the magnetic resonance induced in the capacitive

portion of the unit cell, leading dominantly to the dielectric loss [11]. It is well known that the meta-atoms, such as cut-wire pairs (CWPs) and split-ring resonators, produce two fundamental resonances: the magnetic resonance at lower frequencies and the electric resonance at higher frequencies [12, 13]. The electric resonance has not been applied to manipulate the perfect absorber because of inconvenient heat enhancement of the parallel induced currents. However, it becomes necessary to develop MMs that exploit the electric effect. The expected broadband of absorption and the advantage of parallel induced currents can be noticeable properties of electric-resonance-induced perfect absorbers. The electric resonance was mentioned in [14], but the mechanism was not clarified and property control was not obtained. Recently, by controlling the dispersion of an MM, Ye *et al* achieved PA at both the electric and magnetic resonances,[15] but this is restricted more or less for practical

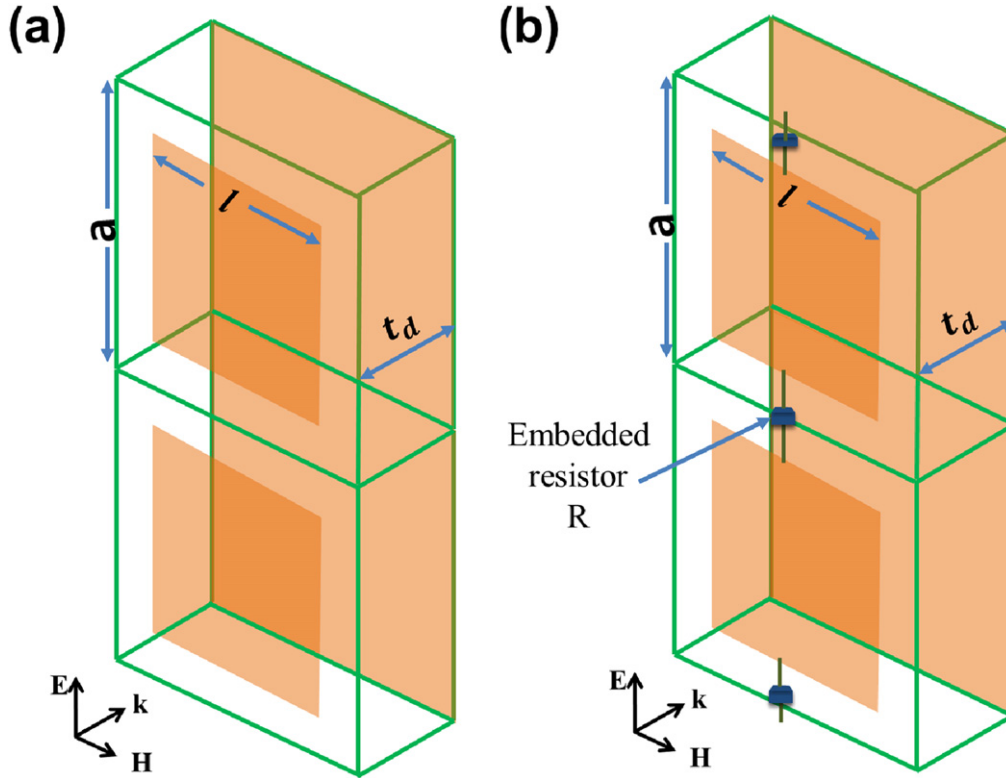


Figure 1. Design of the unit cell (a) without and (b) with embedded resistors.

applications owing to the multilayer structure. In this paper, we investigated the MM PA using a chip resist to provide not only magnetic resonance, but also electric resonance. A simple conventional CWP-like structure was designed, but with embedded resistors at the positions of equivalent electric capacitors to observe the absorption peaks at both magnetic and electric resonances. We realized the triple-band MM PA, which was both numerically and experimentally demonstrated. The origin of triple-band absorption is also clarified.

We introduce a simple but powerful unit cell, shown in figure 1, consisting of three layers: metallic squares connected by two resistors (figure 1(b)) at the front and a metallic plane at the back, separated by a dielectric layer. The unit cell has periodic dimensions of $a = 11$ mm in the E - H plane and $t_d = 0.4$ mm in the k direction. The size of the metallic square is $l = 9$ mm. Chip resistors of 200Ω were attached on conducting straps using the surface mounting technique with solder. The numerical simulations were performed with a commercial software, CST Microwave Studio, based on the finite integration technique [16]. To calculate the S-parameters, the unit cell was set to experience periodic boundary conditions in the E - H plane, and open for the k direction. The transverse-electromagnetic mode of a normally-incident EM wave was polarized so that the electric fields and magnetic fields were configured as in figure 1(a). The metal was copper, with a conductivity of $5.8 \times 10^7 \text{ S m}^{-1}$, and the dielectric layer was FR-4, with a dielectric constant of 4.3 and a loss tangent of 0.025. In case of the conventional MM absorbers, the EM wave was blocked owing to the back metallic plane.

Therefore, the absorbed power, $A(\omega)$, is related to the reflected power, $R(\omega)$, and the reflected coefficient, S_{11} , by $A(\omega) = 1 - R(\omega) = 1 - |S_{11}|^2$. For the experimental process, the PA structure was fabricated using a conventional printed-circuit-board process with copper patterns ($36 \mu\text{m}$ thick) on both sides of a dielectric substrate. The reflection measurements were performed in free space using a Hewlett-Packard E8362B network analyzer. To avoid the near-field effects, the height of the system and the distance between the antennas and the sample were set at 1.5 m and 0.49 m, respectively. The source and the receiver horns were each inclined at an angle of 5° with respect to the normal direction of the sample surface.

Since the thickness of the dielectric layer is much less than the square size ($t_d \ll l$), as seen in figure 1, the resonance modes for only the lower frequency can be derived by [17]

$$k_{nm} = \frac{\omega_{mn} \sqrt{\epsilon}}{c} = \frac{\pi}{l} \sqrt{n^2 + m^2}, \quad (1)$$

where n, m are integers (0, 1, 2...), and $n^2 + m^2 \neq 0$. $\omega_{mn} = 2\pi f_{mn}$, where $f_{mn} = \frac{c\sqrt{n^2 + m^2}}{2l\sqrt{\epsilon}}$ are the resonance frequencies of the classical patch antenna. First, we elucidated the properties of the MA without connecting the chip resistor, as depicted in figure 2. Two absorption peaks are evident: the first peak with an absorption of 94% (at 7.2 GHz), and the second one with an absorption of 98% (at 18.7 GHz). The experiment result is in agreement with the simulation. To understand the mechanism of two resonances, figures 2(c) and (d) present the distributions of the surface current at those

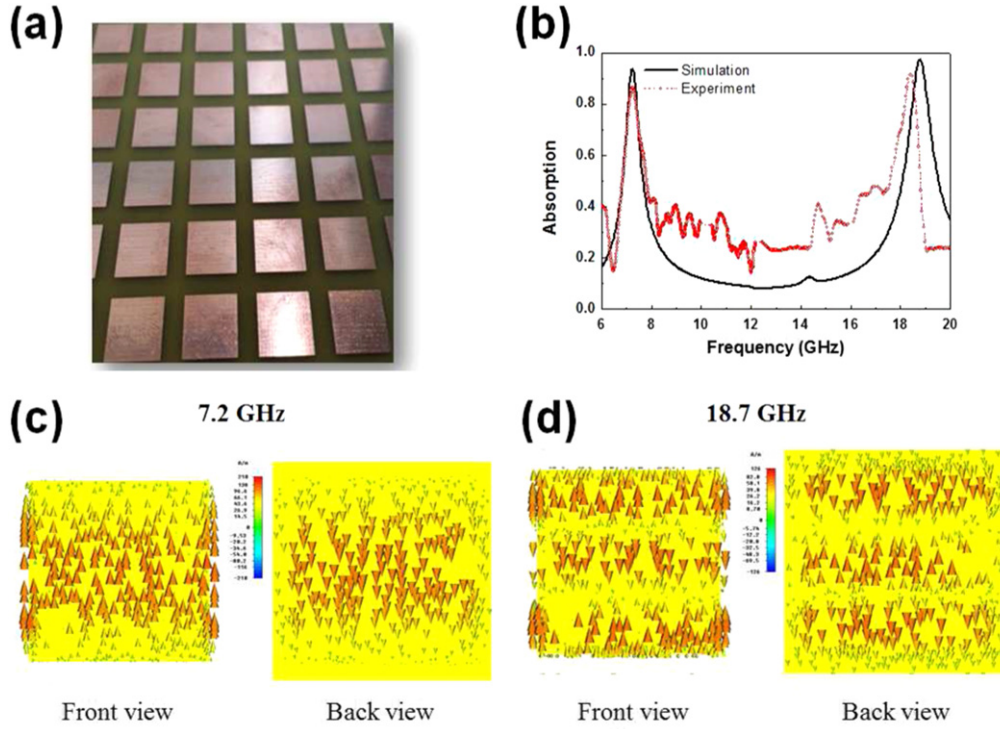


Figure 2. (a) Photograph of the fabricated samples without connecting resistors. (b) Simulated and experimental frequency-dependent absorption for the MA without connecting resistors. (c) and (d) Induced surface currents at the two resonance frequencies.

frequencies. The antiparallel currents at the front and back plates at 7.2 GHz indicate that the absorption is induced by the fundamental magnetic resonance ($n = 1, m = 0$). On the other hand, the surface currents at 18.7 GHz are composed of three sub-anti parallel currents, which correspond to the third-harmonic magnetic resonance ($n = 3, m = 0$) [13, 18]. For the next investigation, we connected the two unit cells with a chip resistor, as in figure 1(b). Interestingly, an absorption peak appears additionally at 13 GHz, and the total power absorption turns out to be higher than 90% in a band of 1.3 GHz from 12.3 to 13.6 GHz in both the simulated and experimental results. In comparison with two other magnetic resonance peaks (with the bandwidth of 0.4 and 0.6 GHz at 7.2 and 17.2 GHz, respectively), the additional absorption peak turns out to have broadband properties (figure 3(b)). To understand the mechanism, the distribution of surface current around the new absorption peak (at 13.6 GHz, slightly away from the peak position of 13 GHz) is shown in figure 3(c), revealing that the surface currents at the corners of the front and the back plates are antiparallel. At the same time, the strong parallel currents at the two edges of the front and back plates indicate that the absorption is induced by the electric resonance and can be broad in frequency. Consequently, the mechanism of the absorption peak at 13.6 GHz is elucidated to be a mixture of the magnetic and the electric resonances.

The resistor, basically, plays an important role in tuning the impedance of the MM surface to match that of the air, but it does not influence the resonance frequency. Based on the calculation method in [19], we can calculate the inductor-capacitor (LC)-circuit properties of the square structure. The

magnetic resonance can be calculated by

$$f_m \approx \frac{c}{2\pi w \sqrt{\epsilon_r c_1}}. \quad (2)$$

$\epsilon_r = 4.3$, c is the speed of light, and c_1 is a numerical factor for a range of $0.2 \leq c_1 \leq 0.3$. The electric resonance is calculated by

$$f_e \approx \frac{c \sqrt{\frac{b}{td}}}{2\pi \sqrt{\epsilon_r w g(w)}}. \quad (3)$$

$g(w)$ is a function which, for $w \rightarrow 0$, behaves as $-\ln(w)$, and b is the distance between two neighboring squares. In [20], the third-order resonance is responded to by multiple localized surface plasma; in other words, the third-order resonance can be expressed by

$$f_{n=2} \approx 3f_m. \quad (4)$$

From equations (2)–(4), the magnetic, electric, and third-order resonance frequencies are nearly unchanged even when we add a resistor, R , to our structure, the impedance of the LC circuit is changed. The impedance-matching frequency is also changed, which slightly shifts the absorption frequency. Figure 4 shows the absorption spectra for various resistance values. When the resistance is equal to 0 (no resistor), the electric resonance erupts around 14 GHz but with very low absorption; the EM wave is reflected because of the mismatched impedance with the air. When the resistance increases, as previously mentioned, the impedance is matched with the air around the electric resonance, and the EM wave can be absorbed.

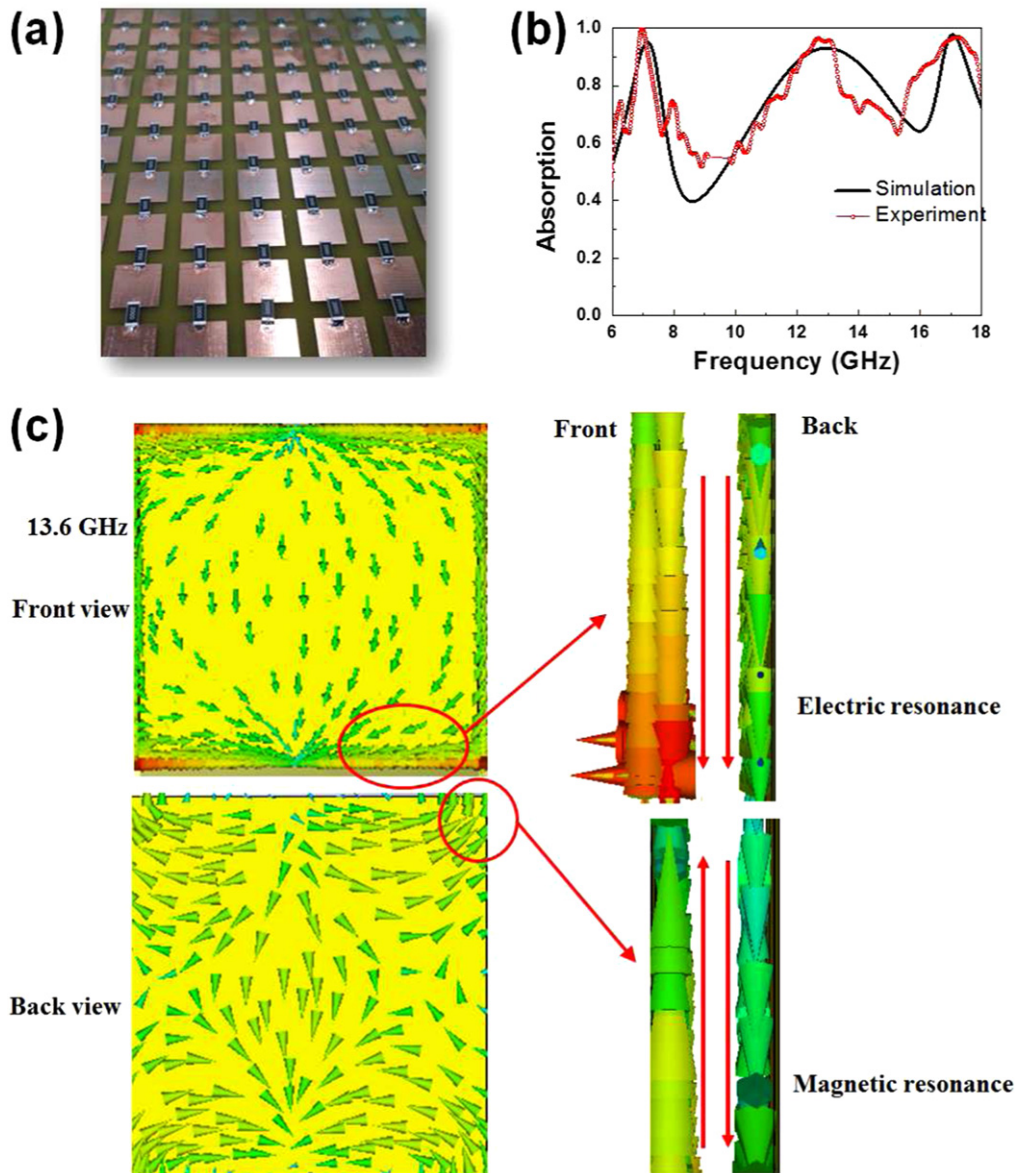


Figure 3. (a) Photograph of the fabricated samples with connecting resistors. (b) Simulated and experimental frequency-dependent absorption for the MA with connecting resistors. (c) Induced surface currents around the electric resonance frequency.

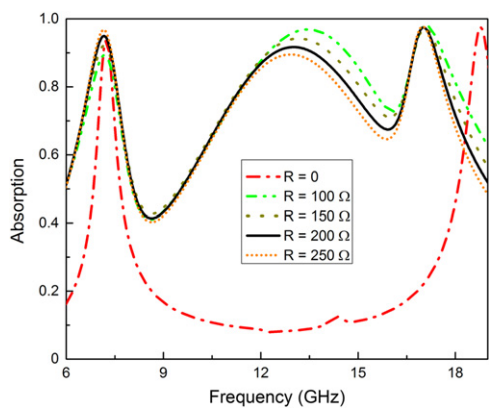


Figure 4. Absorption spectra of MA structure without and with connected resistors, simulated by changing the resistance.

According to figure 4, the magnetic resonance is nearly unchanged, but the third-harmonic peak is more sensitive since the high-order resonance shifts from 18.7 to 17.2 GHz.

To have a deeper understanding of the nature of the additional absorption band, the simulated transmission of an MA without the back metallic plane is presented in figure 5(a). The fundamental and third-harmonic magnetic resonances no longer exist owing to the absence of the metallic plane, which provides the anti parallel currents for the magnetic resonance. The MM structure in figure 5(a) can yield only an electric resonance at 14 GHz, which is very close to the new absorption band in figure 3(b). Therefore, the absorption band is due to the electric resonance which is associated with the effect of the resistors, making the MA impedance match with the air, as shown in figure 5(b). When the impedance of the structure matches with the air, the EM wave propagates through the MA surface without reflection

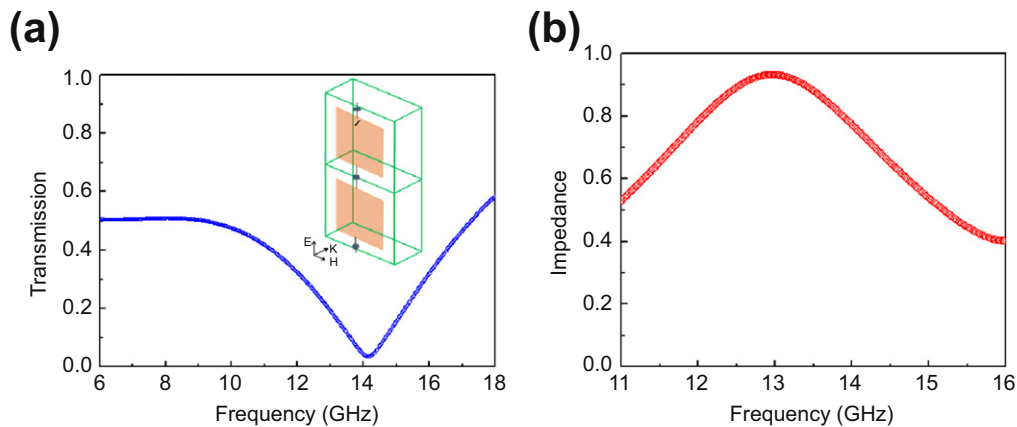


Figure 5. (a) Transmission spectrum of the MA structure without metallic plane. (b) Surface-impedance spectrum in the vicinity of electric resonance frequency.

and is dissipated by the electric dipole mode. The surface impedance was retrieved from the S-parameters, as in [21]. This result demonstrates that both the electric resonance and the magnetic resonance can induce the PA. Our research could lead us to make a device with broadband absorption, and to apply the infrared and the optical bands together with the recent research on optical nanocircuits [22].

A triple-band MA was numerically and experimentally demonstrated by integrating resistors. The MA can be obtained not only by the magnetic resonances, but also by the electric resonances. The combination of electric resonance and resistors leads to the impedance matching of the MA with the air, which yields another high absorption at the electric resonance. Our work promises advanced applications, especially in broadband absorption devices.

Acknowledgments

This work was supported by the ICT R&D Program of the MSIP/IITP, Korea (KCA-2013-005-038-001), and the NRF fund by MSIP, Korea (2011-0017605).

References

- [1] Shalaev V M 2007 *Nat. Photon* **1** 41
- [2] Driscoll T, Kim H-T, Chae B-G, Kim B-J, Lee Y-W, Jokerst N M, Palit S, Smith D R, di Ventra M and Basov D N 2009 *Science* **325** 1518
- [3] Kabashin A V, Evans P, Pastkovsky S, Hendren W, Wurtz G A, Atkinson R, Pollard R, Podolskiy V A and Zayats A V 2009 *Nat. Mater.* **8** 867
- [4] Li G, Chen X, Li O, Shao C, Jiang Y, Huang L, Ni B, Hu W and Lu W 2012 *J. Phys. D: Appl. Phys.* **45** 205102
- [5] Aydin K, Ferry V E, Briggs R M and Atwater H A 2011 *Nat. Commun.* **2** 517
- [6] Urzhumov Y and Smith D R 2011 *Phys. Rev. B* **83** 205114
- [7] Service R F and Cho A 2010 *Science* **330** 1622
- [8] Landy N I, Sajuyigbe S, Mock J J, Smith D R and Padilla W J 2008 *Phys. Rev. Lett.* **100** 207402
- [9] Wang B X, Wang L L, Wang G Z, Huang W Q, Li X F and Zhai X 2014 *IEEE Photon. Technol. Lett.* **26** 111
- [10] Wang B X, Wang L L, Wang G Z, Huang W Q, Li X F and Zhai X 2014 *J. Lightwave Technol.* **32** 1183
- [11] Hao J, Wang J, Liu X, Padilla W J, Zhou L and Qiu M 2010 *Appl. Phys. Lett.* **96** 251104
- [12] Dolling G, Enkrich C, Wegener M, Zhou J F, Soukoulis C M and Linden S 2005 *Opt. Lett.* **30** 3198
- [13] Tung N T, Thuy V T T, Park J W, Rhee J Y and Lee Y P 2010 *J. Appl. Phys.* **107** 023530
- [14] Ding F, Cui Y, Ge X, Jin Y and He S 2012 *Appl. Phys. Lett.* **100** 103506
- [15] Ye D, Wang Z, Xu K, Li H, Huangfu J, Wang Z and Ran L 2013 *Phys. Rev. Lett.* **111** 187402
- [16] <http://cst.com>.
- [17] Balanis C A 1997 *Antenna Theory: Analysis and Design* (New York: Wiley)
- [18] Yoo Y J, Kim Y J, Tuong P V, Rhee J Y, Kim K W, Jang W H, Kim Y H, Cheong H and Lee Y P 2013 *Opt. Express* **21** 32484
- [19] Zhou J, Economou E N, Koschny T and Soukoulis C M 2006 *Opt. Lett.* **31** 3620
- [20] Tuong P V, Park J W, Lam V D, Jang W H, Choi E H, Nikitov S A and Lee Y P 2012 *J. Lightwave Technol.* **30** 3451
- [21] Chen X, Grzegorzczak T M, Wu B-I, Pacheco J and Kong J A 2004 *Phys. Rev. E* **70** 016608
- [22] Liu N, Wen F, Zhao Y, Wang Y, Nordlander P, Halas N J and Al A 2013 *Nano Lett.* **13** 142